Sains Malaysiana 52(8)(2023): 2309-2322
http://doi.org/10.17576/jsm-2023-5208-11

Examining Solar Flare Effects on Earth's Ionosphere using Ground-Based Measurements

(Pengkajian Kesan Nyalaan Suria terhadap Ionosfera Bumi menggunakan Pengukuran Dasar)

Nurul Shazana Abdul Hamid[1,2,*], Raja Adibah Raja Halim[1], Idahwati Sarudin[3], Akimasa Yoshikawa[4,5] & Akiko Fujimoto[6]

[1]Department of Applied Physics, Faculty of Science and Technology, Universiti Kebangsaan Malaysia, 43600 UKM Bangi, Selangor, Malaysia
[2]Space Science Centre (ANGKASA), Institute of Climate Change, Universiti Kebangsaan Malaysia, 43600 UKM, Bangi, Selangor, Malaysia
[3]School of Physics, Universiti Sains Malaysia, 11800 USM, Penang, Malaysia
[4]Department of Earth and Planetary Sciences, Faculty of Sciences, 33 Kyushu University, 6-10-1 Hakozaki, Higashi-ku, Fukuoka 812-8581, Japan
[5]International Research Center for Space and Planetary Environmental Science (i-SPES), Kyushu University, 819-0395 Fukuoka, Japan
[6]Department of Artificial Intelligence, Faculty of Computer Science and Systems Engineering, Kyushu Institute of Technology, 680-4, Kawazu, Iizuka, Fukuoka 820-8502, Japan

Received: 28 January 2023/Accepted: 2 August 2023

ABSTRACT

This study investigated the simultaneous effects of solar flares (SFs) on both the D and E layers of Earth's ionosphere. The analysis focused on the M and X-class SFs that occurred during the 24th solar cycle as these two classes of SFs are known to produce significant effects on Earth's environment, particularly during the daytime period. The data utilized to detect the SF events in this study were ground-based magnetometer data from the equatorial regions. Effects of the selected SF events on the E layer were investigated based on the EUEL index constructed using the geomagnetic data. Meanwhile, the changes in the strength of radio VLF signals in the D ionospheric layer during the selected SF events were monitored using Sudden Ionospheric Disturbance (SID) data. Two case studies were performed which consisted of four SF events from a total of 23 events that were detected by geomagnetic data during the period of study. Further analysis on the selected SF events showed the common effects of SFs on the D layer, which is the increment on the VLF signal measured from the SID stations although a different response was detected in the EUEL index variations. This indicates that the VLF signal always shows an increment even though a decrement in the ionization of the E layer occurs as a result of the SF events. The difference in responses could be attributed to the distinct changes in electron density of both layers during the SF occurrence. Further studies are needed to elucidate the underlying mechanism responsible for this unique response, utilizing appropriate parameters such as total electron content, as well as the electron density data to thoroughly analyze the ionospheric response during SF events.

Keywords: EEJ current; geomagnetic field; SID; solar flare; VLF signal

ABSTRAK

Penyelidikan ini mengkaji kesan nyalaan suria (SF) secara serentak pada kedua-dua lapisan D dan E ionosfera Bumi. Analisis memfokuskan kepada SF kelas M dan X yang berlaku semasa kitaran suria ke-24 kerana kedua-dua kelas SF ini menghasilkan kesan yang ketara ke atas persekitaran Bumi, terutamanya pada waktu siang. Data yang digunakan untuk mengesan kejadian SF dalam kajian ini ialah data magnetometer cerapan dasar dari rantau-rantau khatulistiwa. Kesan kejadian SF yang dipilih pada lapisan E telah dikaji berdasarkan indeks EUEL yang dibina menggunakan data medan geomagnet tersebut. Sementara itu, data Gangguan Ionosfera Mendadak (SID) digunakan untuk memantau

perubahan kekuatan isyarat radio VLF pada lapisan D ionosfera untuk kejadian SF yang terpilih. Dua kajian kes telah dilakukan yang terdiri daripada empat kejadian SF daripada 23 peristiwa yang dikesan oleh data geomagnet sepanjang tempoh kajian. Analisis lanjut mengenai kejadian SF terpilih telah memerhatikan kesan umum SF pada lapisan D iaitu kenaikan pada isyarat VLF yang diukur dari stesen SID walaupun tindak balas berbeza dikesan dalam variasi indeks EUEL. Ini menunjukkan bahawa isyarat VLF sentiasa menunjukkan kenaikan walaupun pengurangan dalam pengionan lapisan E terjadi kesan daripada kejadian SF. Perbezaan dalam tindak balas ini boleh disebabkan oleh perubahan yang berbeza dalam ketumpatan elektron pada kedua-dua lapisan semasa berlakunya kejadian SF. Kajian lanjut diperlukan untuk menerangkan mekanisme tindak balas unik ini dengan menggunakan parameter yang sesuai seperti jumlah kandungan elektron serta data ketumpatan elektron untuk menganalisis secara menyeluruh akan tindak balas ionosfera semasa kejadian SF.

Kata kunci: Arus EEJ; isyarat VLF; medan geomagnet; nyalaan suria; SID

Introduction

Solar flares (SFs) refer to the sudden release of huge amounts of energy from the Sun toward our planet with significant increase in extreme ultraviolet (EUV) and X-ray fluxes during the short period (Le et al. 2007). This space weather event interacts with Earth's atmosphere through the large emission of electromagnetic radiation. The radiation is emitted across the entire electromagnetic spectrum and is responsible for ionospheric irregularities. Consequently, the radiation released is capable of interfering with communication radio on Earth. Another remarkable space weather event is called coronal mass ejection (CME) which involves the huge release of plasma and magnetic fields from the Sun's corona layer. CME produces a huge impact on Earth such as geomagnetic storms which are temporary interference of Earth's magnetosphere caused by the interactions of solar storms with the Earth's magnetic field (Sengupta 1980). The release of SFs is sometimes accompanied by CME, where according to Kahler (1992), for SFs that occur over a long duration, the probability that both would be present together is high. Nonetheless, both are able to occur individually without being accompanied by each other. Additionally, Qian and Woods (2021) reported that the phenomenon of SF and CME can produce solar radio bursts. Hence, there is the possibility that the type of solar radio eruption released is capable of influencing the effects of SFs on Earth's ionospheric layer.

SF events are classified based on the strength of X-rays in the wavelength range 1 Angstrom to 8 Angstrom. There are five major classes of SF, namely A, B, C, M and X. However, only effects of three major classes of SF, namely C, M and X are strong enough to be detected on Earth. Class X is the strongest SF and it can trigger radio blackouts throughout the world and create prolonged radiation storms. Meanwhile, class M is an SF with a moderate X-ray strength that can cause brief radio blackouts that affect Earth's polar regions and create minor radiation storms. In contrast, SFs with class C classification is known to have weak X-ray strength and very few of its effects can be detected on Earth.

SFs can affect the geomagnetic field data by increasing ionization mainly in the E layer, partially in the D layer, and occasionally in the F layer of Earth's ionosphere (Das, Pallamraju & Chakrabarti 2010; Sengupta 1970). The temporary geomagnetic interference in daylight hemispheres due to SF occurrence is known as the 'solar flare effect' or geomagnetic crochets (Annadurai, Hamid & Yoshikawa 2019; Yamazaki et al. 2009). The strength of the SF can be identified via data from the GOES satellite which can be used to verify the geomagnetic crochet observed. Geomagnetic crochet is divided into two, namely positive crochet (sudden current increase) and negative crochet (current decrease). Annadurai et al. (2018) in their study demonstrated the existence of positive crochet and negative crochet based on the ground-based magnetometer data measured at several locations around the world with respect to SF events during the period of 2008 – 2018. These effects are related to the E layer of the ionosphere since geomagnetic data measured at the equatorial regions are greatly affected by the currents flowing in the dayside ionosphere which are known as equatorial electrojet current (EEJ) and Sq current (Hamid et al. 2021; Ismail et al. 2021).

Several recent studies have carried out assessments on SF events and its effect on the D layer using ground-based observations such as magnetometer measurement (Grodji et al. 2021), sudden ionospheric monitoring

(Ugwu, Okechukwu & Udoka 2021), GPS observation (Singh et al. 2020), and ionograms (Curto et al. 2018). Enhanced X-ray fluxes from SF events can cause sudden increase of ionization in Earth's ionosphere, up to the lowest D region, known as sudden ionospheric disturbances (SID). The very low frequency (VLF) radio signal strength data recorded by the receiver station is capable of detecting the SF effects on the D-layer ionosphere (Natras, Horozovic & Mulic 2018). However, the level at which the X-ray ionization becomes dominant depends on the level of solar activity. This current study sought to complete the void of past studies by comparing SF effects on the different layers of the ionosphere, namely the D and E layers of the ionosphere as many of the past studies tend to investigate the effect of each layer separately. Accordingly, the simultaneous effects of SFs on both the D and E layers of Earth's ionosphere were examined in this study based on selected strong SF events. In this work, the effects of four SF events based on the data availability of ground-based magnetometer and SID measurements in the same region of observation are presented.

Method of Analysis

The method of analysis began by identifying SF events using satellite measurements. Subsequently, the impact of SF on the E layer was determined through the analysis of geomagnetic data of EUEL index, which represented the EEJ current. Similarly, the influence of SF on the D layer was investigated by analyzing the VLF data.

Analysis of GOES Data

In this study, the SF observation information was obtained from the website of Lockheed Martin Solar and Astrophysics Laboratory (LMSAL). The information provided on the website includes the date of each day, start time, end time, number of events for each class of SF and the biggest event that ever happened. There is also information about the active area (AR), namely the location of the source of the SF occurrence as well as the surface image of the Sun during the occurrence of the SF (Zhang et al. 2011). Although the data archive from the LMSAL website provides complete data about SF events that occurred on the day of the incident, raw data of X-ray flux from the Geostationary Environment Operational Satellite (GOES) is still required to verify the SF data obtained from the LMSAL website. Moreover, GOES satellites provide data at two wavelengths of 0.1 nm up to 0.8 nm and 0.05 nm to 0.4 nm. A shorter wave reading of 0.05 nm to 0.4 nm gives higher accuracy than long reading waves of 0.1 nm to 0.8 nm (Annadurai, Hamid & Yoshikawa 2019). For this study, SFs for M class and above were chosen to investigate the effects of the SFs on the D and E layers of Earth's ionosphere. This is because the SFs below M class are not strong enough to reach and affect Earth's environment (Natras, Horozovic & Mulic 2018).

Geomagnetic Data

In this study, the geomagnetic northward component data (H-component) were used to detect SF events from the ground level after SF selection was performed based on LMSAL and GOES data. Figure 1 illustrates the ground-based magnetometer instruments located at the stations along the geomagnetic equator from the network of Magnetic Data Acquisition System (MAGDAS) that were used. The stations are located in the South American, South African, and Southeast Asian sectors, and their details are listed in Table 1. However, it is important to note that there is the possibility that these ground measurements may be incapable of detecting certain SF events since there is a large gap between continents as indicated by the square yellow area in Figure 1. The SF event may be undetected if this area does not face daylight during the period of the SF event since no magnetometer station is located there.

After identifying the observable SF events based on the ground H-component data, observation of Kp and Dst indices were performed before conducting the analysis to determine whether the analysis of SF effects on Earth's ionospheric layers could be conducted. This is crucial in order to clarify the existence of geomagnetic storms which can greatly mask the effects of SFs. Additionally, further analysis on EEJ current was only possible on dates when no geomagnetic storm occurred, namely on quiet days, which were indicated by the low Kp values ($Kp \leq 3$) and $Dst \leq -50$ nT.

Not all SF events are able to produce significant effects on ionospheric conductivity (Shah, Abdul Hamid & Yoshikawa 2021). The analysis of SF effects on EEJ current was further carried out on selected dates that fulfilled the SF and quiet day conditions. The EUEL index was derived from the raw geomagnetic data to represent the variation of the EEJ current flowing in the E-layer region (Hamid et al. 2013; Uozumi et al. 2008).

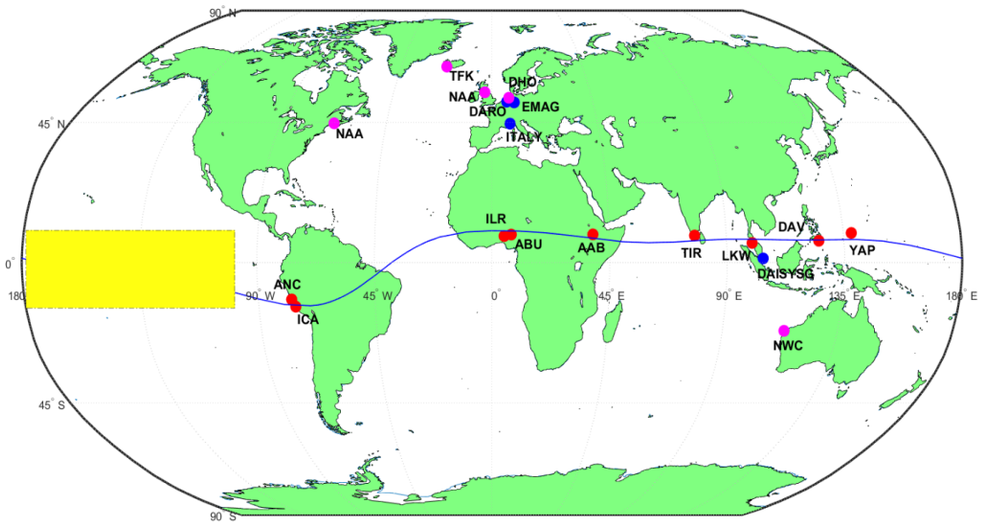

FIGURE 1. Distribution map of the ground-based stations used in this study. Red bullets represent the magnetometer stations while blue and purple bullets indicate the location of the SID receiving and transmitting stations, respectively

TABLE 1. Details of the magnetometer stations used in this study

Station name (Code)	Country	Geographic coordinate (°)		Geomagnetic coordinate (°)	
		Latitude	Longitude	Latitude	Longitude
Addis Ababa (AAB)	Ethiopia	9.04	38.77	5.41	112.54
Abuja (ABU)	Nigeria	8.99	7.39	-0.54	81.31
Ancon (ANC)	Peru	-11.77	-77.15	-2.11	355.57
Davao (DAV)	Philippine	7.00	125.40	-2.22	197.90
Ilorin (ILR)	Nigeria	8.50	4.68	10.50	78.90
Langkawi (LKW)	Malaysia	6.30	99.78	-3.30	172.44
Tirunelveli (TIR)	India	8.70	77.80	0.25	150.80
Yap Island (YAP)	FSM	9.50	138.08	1.14	210.25
Ica (ICA)	Peru	-14.09	-75.74	-4.42	356.97

The index is divided into two, namely the EU and the EL. The EU index represents the EEJ current, and the EL index represents the counter of the EEJ current, namely the CEJ current (Rosli et al. 2022). The EUEL index from the ground stations was investigated to identify the type of SF effect, in terms of whether it caused increment or decrement in the EEJ currents.

VLF RADIO SIGNAL ANALYSIS

Data from the SID monitor that recorded the VLF radio signal strength at every five seconds was used to observe the SID events. SID monitors consist of antennas, pre-amplifiers, and computers with sound cards. Loop-like antennas serve as a receiver of VLF signals from

various transmitter stations reflected from the ionosphere. The loop antenna covers the circuit inductors-capacitors that are capable of detecting VLF signals (McRae & Thomson 2000). In this study, the VLF radio signal data supplied by the Stanford Solar Center were used. Information provided by this data provider consists of the date, time for every five seconds in UT time, and the VLF signal strength data received. The SID receiving and transmitting stations were selected based on the same coverage area as the magnetometer stations, where the receiving and transmitting stations are illustrated in Figure 1 using blue and purple bullets, respectively. The details of each station are presented in Table 2. In the analysis of the SF effects on the D-layer region represented by the VLF signal variation, the data selection was made based on the availability of the EUEL index which represents the variation of the EEJ's current intensity flowing in the E layer of the ionospheric region. This was done to ensure that the analysis performed would be able to reflect the simultaneous responses of the SF effects on both layers.

RESULTS AND DISCUSSION

SOLAR FLARE OBSERVATION

In this study, analysis on solar flare (SF) occurrence was performed on the observational data from January 2008 to May 2018. Figure 2(a) is an example of an X-ray flux reading from the GOES-15 satellite showing the X1.9 class SF event (shaded region) that occurred on 24 September 2011. A total of 59 events of strong SFs from classes of M8 and above were identified throughout the ten-year period of observation. These strong SF events were further analyzed to identify whether their presence is detectable or undetectable on the ground measurement magnetometer data from the stations listed in Table 1.

Based on the analysis performed, the dates of 36 SF events that were undetected from the observation of H component data were identified, and these dates are listed in Table S1. Table S1 also lists the recorded start time, stop time and peak time of the SF events. The maximum value of Kp and range of Dst indices were recorded to verify the influence of geomagnetic storms on the observational data on the event days. The days when geomagnetic storms occurred were then recorded as 'Storm' under the category 'Condition'. The term 'Night' represents the condition when no observatory stations are located on the dayside (yellow area in Figure 1); thus, the SF effects were undetectable by the ground measurement. Additionally, failure to detect SF events from the ground measurements could also be due to the position of Earth which was not parallel or facing the origin of the SF events on the Sun's surface, or any other possible reasons.

TABLE 2. Details of the SID receiver and transmitter stations used in this study

Location	Country	Code	Geographic coordinate (°)	
			Latitude	Longitude
SID Receiver stations				
Bonn	Germany	EMAG	51.53	9.92
Singapore	Singapore	DAI-SYSG	1.36	103.80
Fasano	Italy	ITALY	44.53	7.72
Dusseldorf	Germany	DARO	51.76	6.61
VLF Transmitter stations				
Cutler, ME	U.S. Navy	NAA	44.64	-67.28
Harold E. Holt	Australia	NWC	-21.81	114.16
Keflavic	Iceland	TFK	63.85	-22.46
Rhauderfehn	Germany	DHO	53.07	7.61
Anthorn	United Kingdom	GBZ	54.91	-3.27

These kinds of conditions were marked as 'No effect'. However, it is beyond the scope of the current study to identify the causes. The illustration for the distribution of these conditions (undetectable, U) over the years is presented in Figure 3.

Further analysis on the effects of SFs on both the D and E layers were performed on 23 out of the 59 events where the presence of SFs was detected by geomagnetic data. Table S2 lists the dates of these events while the distribution (detectable, D) is presented together with the undetectable SF events in Figure 3. Based on Figure 3, it can be observed that although maximum number of strong SFs happened in the year 2014 (a total of 18 events consisting of 16 undetectable (U) and 2 detectable (D) SF events), the detection of these events by ground-based geomagnetic data was not remarkable for that year. Figure 2(b) represents an example of detectable SF effects (shaded region) in the variation of the H component data from LKW station during the year 2011.

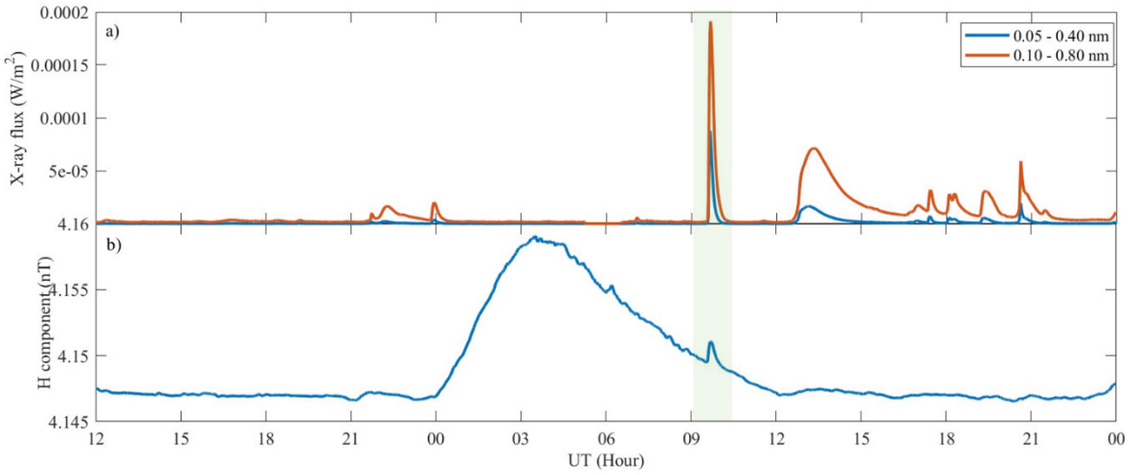

FIGURE 2. Variation of (a) solar X-ray flux from the GOES-15 satellite, and (b) geomagnetic H component data from Langkawi station, LKW on 24 September 2011. Shaded region shows the period when the X1.9 class SF event occurred and was detectable on the H component data

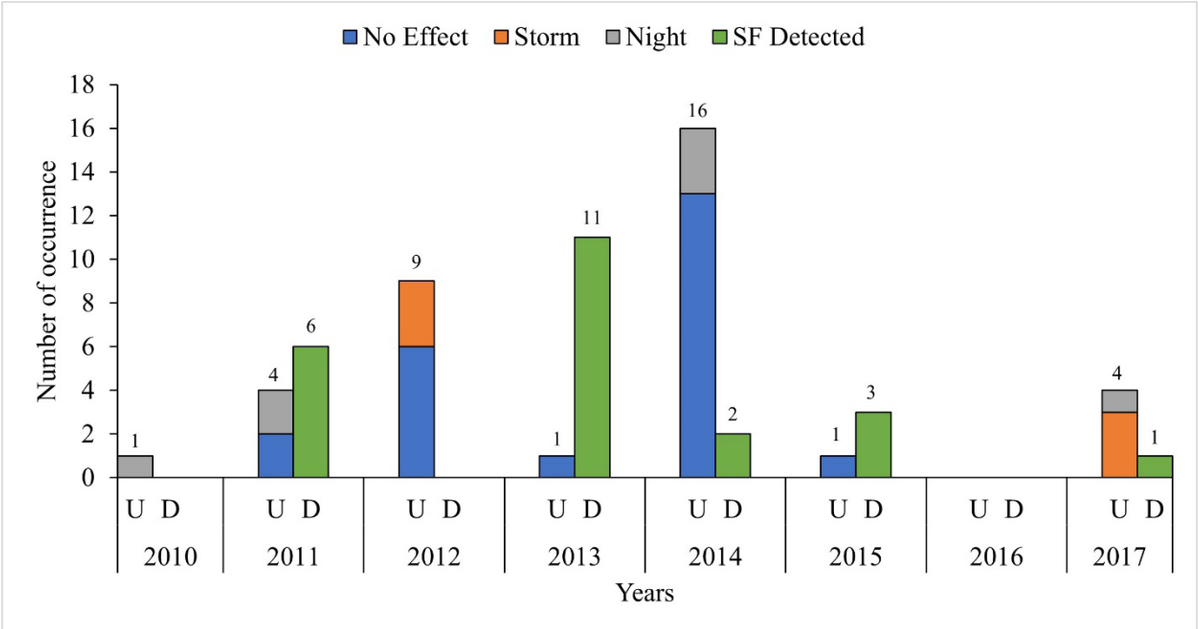

FIGURE 3. Occurrence of SF events that are undetectable (U) and detectable (D) in the ground-based magnetometer data over the years

SOLAR FLARE EFFECTS ON THE D AND E IONOSPHERIC LAYERS

For the analysis to determine the SF effects on the D and E layers of the ionosphere, selected dates were chosen from the 23 dates in which SF events were detectable in the variation of the H component data. Two remarkable effects of SF events on the EEJ current were observed as suggested by previous studies (Annadurai et al. 2018; Sumod & Pant 2019; Zhang et al. 2017), namely increment (Case I) and decrement (Case II) of current density. Two case studies each for Case I and Case II were thus performed. A total of four dates were chosen based on the availability of EUEL and VLF signal data at the same longitude of the observatory region(s). This was performed to ensure the simultaneous effects of SFs at both layers could be obtained.

CASE I - INCREMENT IN THE EEJ CURRENT

Figure 4 shows the variation of the X-ray flux, time series of the EUEL index describing the ionization changes in the E layer as well as the variability of the VLF signal which refers to the response of the D layer. On 11 March 2015, an X2.1 SF was detected at 16:22 UT as shown in Figure 4(a). On this date, no geomagnetic storm occurred as indicated by the low value of the Dst index. The EEJ current readings observed by ABU station showed an increment during the occurrence of the SF where the change in current intensity can be seen in Figure 4(b). The available data of the SID receiver and VLF transmitter stations were plotted and are shown in Figure 4(c). The analysis showed that at the time of the SF event, the readings of the received VLF signal showed significant increment. Effects found in these E and D layers were categorized as a common effect which occurred because of excess radiation during the SF, causing increase in ionization over Earth's ionospheric region as commonly reported by previous studies (Natras, Horozovic & Mulic 2018).

The second case study involved an X1.2 SF event that occurred at 01:48 UT on 15 May 2013 (Figure 5(a)). The Dst index during the day of the event indicated no occurrence of geomagnetic storm. The EUEL data were observed from the ground-based magnetometer station at LKW, and the VLF signal was observed from the SID receiving station of DAISYSG. Figure 5 shows the parallel effect between the EUEL index data and SID receiver observation data where both showed an increase in readings of E and D region measurement during the occurrence of the SF on that day.

Based on Figures 4 and 5, the VLF signal strength observed by all SID receivers showed an increment during the SF events. Ionization at the D-layer altitude was mainly due to daily solar radiation and X-ray flux. Thus, the variation of the VLF signal strength reflected the variation of the ionization applied to the D-layer where it showed a significant increase with the excess radiation due to the SF event during the day (Contreira et al. 2005; Moral, Kalafatoglu Eyiguler & Kaymaz 2013). Comparison between changes of representative measurements of the D and E -layers showed parallel effect of SF exhibited at these two layers.

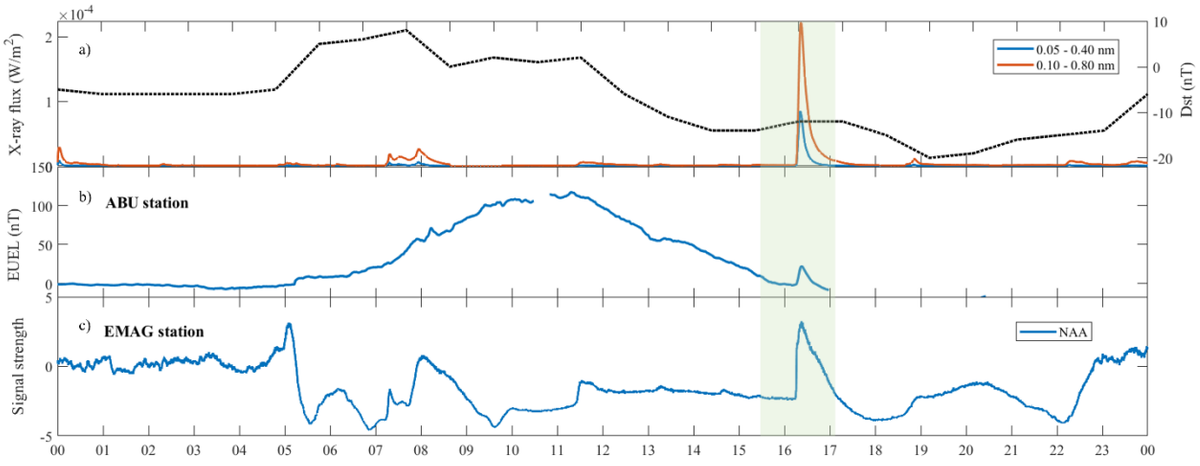

FIGURE 4. (a) X-ray flux observed by GOES-15 satellite on 11 March 2015. (b) EUEL from the magnetometer at ABU station. (c) VLF signal strength from the SID receiver at EMAG station

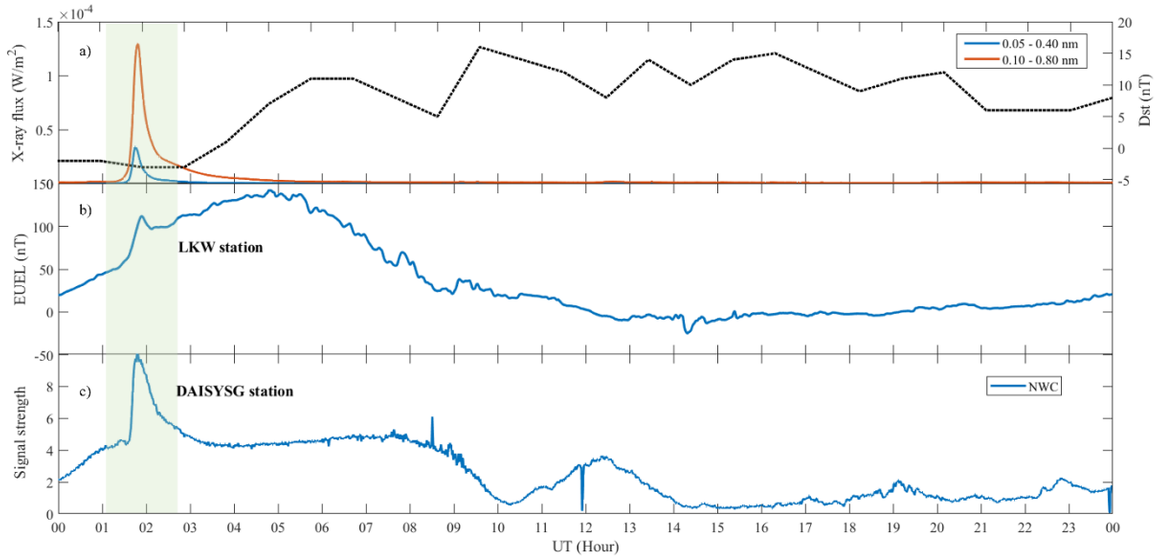

FIGURE 5. (a) X-ray flux observed by GOES-15 satellite on 15 May 2013. (b) EUEL from the magnetometer at LKW station. (c) VLF signal strength from the SID receiver at DAISYSG station

CASE II – DECREMENT IN THE EEJ CURRENT

The analysis then proceeded with the dates showing Case II (E-layer ionospheric current represented by EUEL index showing decrement) for two selected solar flare (SF) events. The analysis began with the event on 9 August 2011 when Case II was observed due to an X6.9 SF event that occurred at 08:05 UT as shown in Figure 6(a). This SF was not accompanied by geomagnetic storm event as indicated by the low value of the Dst index. In this event, the EUEL index from ABU station was used to represent changes in the EEJ current. It can be clearly seen in Figure 6(b) that this SF event caused a decrease in the intensity of the EEJ current which was indicated by the negative value of the EUEL index during the period of the event. Observations of the effect of the SF on the D layer on this date showed an increase in the VLF signal received by the SID receivers at DARO and ITALY stations during the period of the event. The effect can be clearly seen in Figure 6(c) and Figure 6(d).

The analysis then continued by examining the data from the Southeast Asian sector for Case II dated 24 October 2013. During the early hours on this date, an M9.3 SF event occurred which was indicated by the increment in the X-ray flux observed by the GOES-15 satellite at 00:30 UT (Figure 7(a)). The very low Dst index value indicated no occurrence of geomagetic storm during this period. The changes in the EEJ current in this case study were indicated by the small decrement in the EUEL data observed by the ground-based magnetometer at LKW station as shown in Figure 7(b). Although the intensity of the current was lower during the morning hours of local time, changes in the EUEL trend (turning to negative value) could still be seen during the peak time of this SF event. In contrast, the VLF signal received by the SID receiver at the DAISYSG station showed significant increment during the period of the SF event (Figure 7(c)).

During the quiet days when no space weather event occurs, the D layer is dominantly affected by the Lyman-alpha radiation with X-ray flux and gamma rays being minor contributors. However, during the occurrence of SFs, there is a significant increase in radiation. The radiation penetrates directly into the lowest layer of the ionosphere and contributes to Sudden Ionospheric Disturbance or SID for short (Dahlgren et al. 2011; Deshpande, Subrahmanyam & Mitra 1972). SFs cause a significant increase in plasma density at the dayside of the ionosphere which affects the propagation of VLF signals which could be seen in all the selected dates in this study. However, based on the two case studies, the analysis clearly demonstrated that the D and E layers showed different response toward the selected SF events with the former layer exhibiting increment while the later experiencing decrement in the intensity of the paramaters that represent the layers, respectively. Analysis on variations of the EUEL index from different longitude sectors as shown in Figures 6(b) and 7(b) showed the decrease of EEJ current due to the SF events. On the other hand, observations of the plots in Figures 6(c) and 7(c) clearly show that extra ionization due to

the SF events caused an enhancement in the VLF signals, indicating an increase in the electron density of the D layer of the ionosphere. This is a common response of the D layer that has been reported in many previous studies (Kumar & Kumar 2018).

A previous study by Annadurai, Hamid and Yoshikawa (2019) highlighted the unique SF effect of 9 August 2011 which was observed at several dayside equatorial stations in various longitude sectors. One of the suggested possibilities that led to this effect is the influence of the ionospheric D layer. However, in our analysis, the VLF signal on this date showed increment in intensity, representing the common response of the D layer to SF events. Despite the challenges of obtaining simultaneous data from various sources, further studies can be conducted using ionosonde observation events as implemented by Sripati et al. (2013) to further show and confirm the D-layer ionization response toward SF.

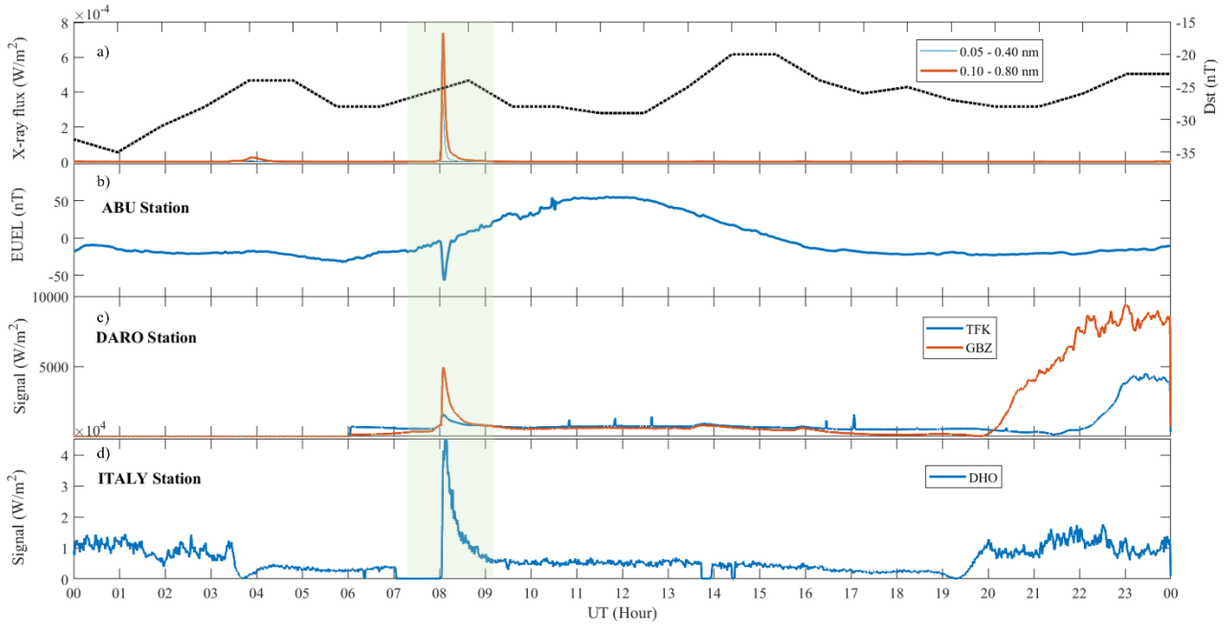

FIGURE 6. (a) X-ray flux observed by GOES-15 satellite on 9 August 2011. (b) EUEL from the magnetometer at ABU station. (c) VLF signal strength from the SID receiver at DARO station. (d) VLF signal strength from the SID receiver at ITALY station

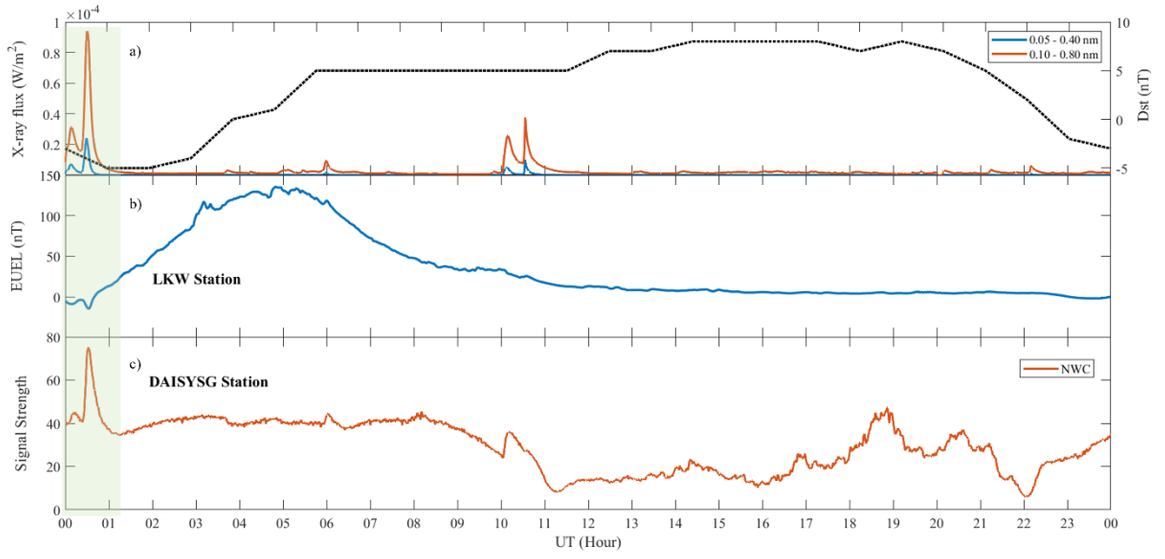

FIGURE 7. (a) X-ray flux observed by GOES-15 satellite on 24 October 2013. (b) EUEL from the magnetometer at LKW station. (c) VLF signal strength from the SID receiver at DAISYSG station

Conclusions

This study has successfully examined the effects of selected SF on the D and E layers of Earth's ionosphere after obtaining the distribution of detectable and undetectable SF events using geomagnetic ground-based data. The effects of SF on the ionospheric EEJ current flowing at the E layer, namely Case I (increment) and Case II (decrement) have been analyzed. The results of this study showed the same response of VLF signal on the D layer was obtained, namely increment was observed during the period of SF events for all the case studies performed. This indicates that the regular or common effects of VLF signal variations were observed regardless of the differences in the E-layer ionization response toward the strong SF events. Future study involving other data sources is suggested to further understand the relation between the D and E layers of the ionosphere during the occurrence of SF events. The observed variation in responses could potentially be attributed to different changes in the electron density of both ionospheric layers during the occurrence of SF events. Thus, one of the proposed data sets involves the measurement of electron density profiles through ionosonde observations. Apart from that, the assessment of total electron content using GPS receiver could be crucial in elucidating the mechanisms underlying this distinct ionospheric response.

Acknowledgements

Special thanks are extended to the Malaysian Space Agency (MYSA) and the MAGDAS Malaysia team for their contribution in the sustainability of the operation of the MAGDAS Langkawi station, Malaysia. This work was funded by the GP-K018967 grant from Universiti Kebangsaan Malaysia. Idahwati Sarudin is supported by Universiti Sains Malaysia through Short-Term Grant with project number 304/PFIZIK/6315730. Akimasa Yoshikawa is supported by JSPS KAKENHI Grant Numbers JP20H01961, JP21K03646, JP21H04518 and JP22K21345. Akiko Fujimoto is supported by JSPS KAKENHI Grant Numbers JP21K03646, JP21H04518. The information of the SF observation was obtained from the Lockheed Martin Solar and Astrophysics Laboratory (LMSAL) website, http://www.lmsal.com/solarsoft/latest_events_archive.htmlr. Meanwhile, the X-ray flux data were obtained from the website https://satdat.ngdc.noaa.gov/sem/goes/. We would like to acknowledge the Stanford SOLAR Center for providing free access to the Sudden Ionospheric Disturbance data (http://sid.stanford.edu/database-browser/).

References

Annadurai, N.M.N., Hamid, N.S.A. & Yoshikawa, A. 2019. Statistical study of equatorial geomagnetic crochets. *AIP Conference Proceedings* 2111(1): 030003.

Annadurai, N.M.N., Hamid, N.S.A., Yamazaki, Y. & Yoshikawa, A. 2018. Investigation of unusual solar flare effect on the global ionospheric current system. *Journal of Geophysical Research: Space Physics* 123(10): 8599-8609.

Contreira, D.B., Rodrigues, F.S., Makita, K., Brum, C.G.M., Gonzalez, W., Trivedi, N.B., Da Silva, M.R. & Schuch, N.J. 2005. An experiment to study solar flare effects on radio-communication signals. *Advances in Space Research* 36(12): 2455-2459.

Curto, J.J., Marsal, S., Blanch, E. & Altadill, D. 2018. Analysis of the solar flare effects of 6 September 2017 in the ionosphere and in the earth's magnetic field using spherical elementary current systems. *Space Weather* 16(11): 1709-1720.

Dahlgren, H., Sundberg, T., Collier, A.B., Koen, E. & Meyer, S. 2011. Solar flares detected by the new narrowband VLF receiver at SANAE IV. *South African Journal of Science* 107(9-10): 1-8.

Das, U., Pallamraju, D. & Chakrabarti, S. 2010. Effect of an x-class solar flare on OI 630nm dayglow emissions. *Journal of Geophysical Research: Space Physics* 115: A08302.

Deshpande, S.D., Subrahmanyam, C.V. & Mitra, A.P. 1972. Ionospheric effects of solar flares-I. The statistical relationship between X-ray flares and SID's. *Journal of Atmospheric and Terrestrial Physics* 34(2): 211-227.

Grodji, O.D.F., Doumbia, V., Amaechi, P.O., Mazaudier, C.A., N'guessan, K., Diaby, K.A.A., Zie, T. & Boka, K. 2021. A study of solar flare effects on the geomagnetic field components during solar cycles 23 and 24. *Journal of Atmosphere* 13(1): 69.

Hamid, N.S.A., Rosli, N.I.M., Ismail, W.N.I. & Yoshikawa, A. 2021. Effects of solar activity on ionospheric current system in the Southeast Asia region. *Indian Journal of Physics* 95(4): 543-550.

Hamid, N.S.A., Liu, H., Uozumi, T. & Yumoto, K. 2013. Equatorial electrojet dependence on solar activity in the Southeast Asia sector. *Antarctic Record* 57: 329-337.

Ismail, W.N.I., Hamid, N.S.A., Abdullah, M., Yoshikawa, A., Uozumi, T. & Radzi, Z.M. 2021. Comparison of EEJ longitudinal variation from satellite and ground measurements over different solar activity levels. *Universe* 7(2): 23.

Kahler, S. 1992. Solar flares and coronal mass ejections. *Annual Review of Astronomy and Astrophysics* 30(1): 113-141.

Kumar, A. & Kumar, S. 2018. Solar flare effects on D-region ionosphere using VLF measurements during low- and high-solar activity phases of solar cycle 24. *Earth Planets Space* 70(1): 29.

Le, H., Liu, L., Chen, B., Lei, J., Yue, X. & Wan, W. 2007. Modeling the responses of the middle latitude ionosphere to solar flares. *J. Atmos. Solar-Terr. Phys.* 69: 1587-1598.

McRae, W.M. & Thomson, N.R. 2000. VLF phase and amplitude: daytime ionospheric parameters. *J. Atmos. Solar-Terrestrial Phys*. 62(7): 609-618.

Moral, A.C., Kalafatoglu Eyiguler, E.C. & Kaymaz, Z. 2013. Sudden ionospheric disturbances and their detection over Istanbul. *2013 6th International Conference on Recent Advances in Space Technologies (RAST)*. pp. 765-768.

Natras, R., Horozovic, D. & Mulic, M. 2018. Strong solar flare detection and its impact on ionospheric layers and on coordinates accuracy in the Western Balkans in October 2014. *SN Applied Sciences* 49: 2019.

Qian, L. & Woods, T.N. 2021. Solar flare effects on the thermosphere and ionosphere. In *Upper Atmosphere Dynamics and Energetics*, edited by Wang, W., Zhang, Y. & Paxton, L.J. American Geophysical Union. pp. 253-274.

Rosli, N.I.M., Hamid, N.S.A., Abdullah, M., Yusof, K.A., Yoshikawa, A., Uozumi, T. & Rabiu, B. 2022. The variation of counter-electrojet current at the southeast Asian sector during different solar activity levels. *Applied Sciences* 12(14): 7138.

Sengupta, P.R. 1980. Solar x-ray control of the D-region of the ionosphere. *Journal of Atmospheric and Solar-Terrestrial Physics* 42(4): 329-335.

Sengupta, P.R. 1970. X-ray control of the E-layer of the ionosphere. *Journal of Atmospheric and Solar-Terrestrial Physics* 32(7): 1273-1282.

Shah, R.A.R.H., Abdul Hamid, N.S. & Yoshikawa, A. 2021. Effect of strong solar flare events on the geomagnetic equatorial region during solar cycle-24. *International Conference on Space Science and Communication, IconSpace*. pp. 298-302.

Singh, A., Rao, S.S., Rathore, V.S., Singh, S.K. & Singh, A.K. 2020. Effect of intense solar flare on TEC variation at low-latitude station Varanasi. *J. Astrophys. Astr.* 41: 19.

Sripati, S., Balachandran, N., Veenadhari, B., Singh, R. & Emperumal, K. 2013. Response of the equatorial and low-latitude ionosphere to an intense X-class solar flare (X7/2B) as observed on 09 August 2011. *Journal of Geophysical Research: Space Physics* 118: 2648-2659.

Sumod, S.G. & Pant, T.K. 2019. An investigation of solar flare effects on equatorial ionosphere and thermosphere using co-ordinated measurements. *Earth, Planets and Space* 71: 125.

Ugwu, E.B.I., Okechukwu, U.D. & Udoka, A.J. 2021. On the effects of solar flare on geomagnetic components across all latitudes during solar minimum and maximum. *Academic Journals: Scientific Research and Essays* 16(3): 42-50.

Uozumi, T., Yumoto, K., Kitamura, K., Abe, S., Kakinami, Y., Shinohara, M., Yoshikawa, A., Kawano, H., Ueno, T., Tokunaga, T., Mcnamara, D., Ishituka, J.K., Dutra, S.L.G., Damtie, B., Doumbia, V., Obrou, O., Rabiu, A.B., Adimula, I.A., Othman, M., Fairos, M., Otadoy, R.E.S. & MAGDAS Group. 2008. A new index to monitor temporal and long-term variations of the equatorial electrojet by MAGDAS/CPMN real-time data: *EE*-Index. *Earth Planets and Space* 60: 785-790.

Yamazaki, Y., Yumoto, K., Yoshikawa, A., Watari, S. & Utada, H. 2009. Characteristics of counter-Sq SFE (SFE*) at the dip equator CPMN stations. *Journal of Geophysical Research* 114: A05306.

Zhang, L., Mursula, K., Usoskin, I. & Wang, H. 2011. Global analysis of active longitudes of solar x-ray flares. *Journal of Atmospheric and Solar-Terrestrial Physics* 73(2-3): 258-263.

Zhang, R., Liu, L., Le, H. & Chen, Y. 2017. Equatorial ionospheric electro-dynamics during solar flares. *Geophysical Research Letters* 44(10): 4558-4565.

*Corresponding author; email: shazana.ukm@gmail.com

SUPPLEMENTARY FILES

TABLE S1. List of solar flare events that were undetected from the observation of ground-based geomagnetic data

Year	Day/Month	SF Class	Time (UT)			Kp Index	Range/value of Dst Index	Condition
			Initial	Final	Peak			
2010	12/02	M8.3	11:19	11:28	11:26	3.00	-22>-21	Night
	15/02	X2.2	01:44	01:56	01:45	2.00	-30>-31	No effect
2011	09/03	X1.5	23:13	23:16	23:23	2.00	-3	Night
	22/09	X1.4	10:29	11:44	11:01	2.00	-9	No effect
	03/11	X1.9	20:16	20:32	20:27	2.00	-26>-28	Night
	23/01	M8.7	03:38	03:59	03:59	5.00	-68>-70	Storm
	27/01	X1.7	17:37	18:56	18:36	3.00	-17>-18	No effect
	05/03	X1.1	02:30	04:43	04:05	3.00	-32>-35	No effect
	07/03	X5.4	00:02	00:40	00:24	4.00	-10>-17	No effect
2012	07/03	X1.3	01:05	01:23	01:14	3.00	-17>-21	No effect
	10/03	M8.4	17:15	18:30	17:44	5.00	-61>-55	Storm
	06/07	X1.1	23:01	23:14	23:08	5.00	-25>-9	Storm
	20/10	M9.0	18:05	18:19	18:14	1.00	-2	No effect
	23/10	X1.8	03:13	03:21	03:17	2.00	9>2	No effect
2013	14/05	X3.2	00:00	01:20	01:11	2.00	15>17	No effect
	01/01	M9.9	18:40	19:03	18:52	3.00	-26>-27	No effect
	07/01	X1.2	18:04	18:58	18:30	3.00	-8>-9	Night
	25/02	X4.9	00:39	01:03	00:49	2.00	-11>-17	No effect
2014	12/03	M9.3	22:28	22:39	22:34	3.00	-1>-6	No effect
	25/04	X1.3	00:17	00:38	00:27	3.00	-21>-20	No effect
	10/06	X2.2	11:36	11:44	11:42	2.00	-7>2	No effect
	10/06	X1.5	12:36	13:03	12:52	2.00	2>6	No effect
	10/09	X1.6	17:21	17:45	17:45	3.00	5>4	No effect

	19/10	X1.1	04:17	05:48	05:01	3.00	-30>-23	No effect
	22/10	X1.6	14:02	14:50	14:28	4.00	-28>-30	No effect
	24/10	X3.1	21:07	21:41	21:40	4.00	-33>-29	No effect
	25/10	X1.0	16:55	17:08	17:08	3.00	-21>-17	No effect
	26/10	X2.0	10:04	11:18	10:56	3.00	-30>-25	No effect
	27/10	X2.0	14:12	15:09	14:47	4.00	-21>-13	Night
	07/11	X1.6	16:53	17:34	17:25	3.00	-4>-6	Night
	20/12	X1.8	00:11	00:55	00:27	3.00	-14>-8	No effect
2015	07/03	M9.2	21:59	22:49	22:00	4.00	-20>-24	No effect
	06/09	X9.3	11:53	12:10	12:02	3.0	17>21	Night
	07/09	X1.3	14:20	14:55	14:36	2.0	13>12	Night
2017	08/09	M8.1	7:40	7:58	7:49	4.00	-87>-85	Storm
	10/09	X8.2	15:35	16:31	16:06	3.00	-19>-20	Night

TABLE S2. List of solar flare events that were detected from the observation of ground-based geomagnetic data

Year	Day/Month	SF	Time (UT)			Kp Index	Range of Dst Index
		Class	Initial	Final	Peak		
2011	30/07	M9.3	02:04	02:12	02:09	1.00	-3>1
	04/08	M9.3	03:41	03:57	03:45	1.00	-1>0
	09/08	X6.9	07:48	08:08	08:05	3.00	-28>-24
	06/09	X2.1	22:12	22:24	22:16	2.00	-8>-5
	07/09	X1.8	22:32	22:44	22:38	1.00	-9
	24/09	X1.9	09:21	09:48	09:40	2.00	-3
2013	13/05	X2.8	15:48	16:16	16:05	2.00	7>12
	15/05	X1.2	01:25	01:58	01:48	1.00	-2>-3
	24/10	M9.3	00:21	00:35	00:30	1.00	-3>-5
	25/10	X1.7	07:53	08:01	08:01	1.00	5>4
	25/10	X2.1	14:51	15:12	15:03	1.00	0>-2
	28/10	X1.0	01:41	02:12	02:03	1.00	7>3
	29/10	X2.3	21:42	22:01	21:54	3.00	-4>2

	05/11	X3.3	22:07	22:15	22:12	1.00	-2>-1
	08/11	X1.1	04:20	04:29	04:26	2.00	-13>-15
	10/11	X1.1	05:08	05:18	05:14	3.00	-28>-25
	19/11	X1.0	10:14	10:34	10:26	1.00	-6>-5
2014	29/03	X1.0	17:35	17:54	17:48	1.00	-4>-3
	11/06	X1.0	08:59	09:10	09:06	2.00	3>1
2015	03/03	M8.2	01:25	01:42	01:35	3.00	-24>-22
	11/03	X2.1	16:11	16:29	16:22	3.00	-14>-12
	05/05	X2.1	22:05	22:15	22:11	2.00	-7>-1
2017	06/09	X2.2	08:57	09:17	09:10	3.00	19>18